



Thermal Properties of Graphene Oxide Prepared from Different Agricultural Wastes



Hebat-Allah S. Tohamy¹, Samir Kamel¹, Mohamed El-Sakhawy^{1*}, Mohamed A. Youssef², Amira E. M. Abdallah², Badawi Anis³

¹Cellulose and Paper Department, National Research Centre, 33 El-Bohouth Str., P.O. 12622, Dokki Giza, Egypt.

²Department of Chemistry, Faculty of Science, Helwan University, Egypt.

³Spectroscopy Department, Physics Division, National Research Centre, 33 El Bohouth Str., P.O. 12622, Dokki Giza, Egypt.

GRAPHENE oxide (GO) extracted from different agricultural wastes such as sugarcane bagasse (SCB), rice straw (RS), lignin (L), mature beech pinewood sawdust (MW) in the presence and absence of ferrocene as a catalyst at 300 °C in a muffle have been prepared, characterized and evaluated by TGA and DTA. TGA decomposition curves of GO showed three decomposition stages for all studied samples except for GO prepared from SCB and MW in the absence of ferrocene, which revealed two decomposition stages. The residual weight of SCB was very low; this indicates its high purity and absence of inorganic residues. The high production of char residue from MW, and L pyrolysis can be ascribed to its lower content of methoxyl group (determined by FTIR). The activation energy (E_a) determined for thermal reduction of GO are found to be from 21.00 to 55.35 kJ/mol. From TGA, it was found that the rate of removal of oxygen-containing functional groups depends on the temperature, which agrees with the experimental findings and thermal degradation kinetics. The free energy change of activation (G) of this system is positive. Consequently, the thermodynamics of GO should be non spontaneous.

Keywords: Graphene oxide, Carbon nanomaterials, Thermal properties, Agricultural wastes, Recycling, Sugarcane bagasse, Rice straw, Lignin, Activation energy (E_a), Thermogravimetric analysis (TGA), Differential thermogravimetric analysis (DTA).

Introduction

Agricultural residues have been used for production of paper, board, and miscellaneous products. Recently pyrolysis of agricultural residues attracted attention for production of graphene and its derivatives [1-2]. Research on carbon nanomaterials have very attractive physical and optical properties which can be employed into a lot of applications such as composite technology, nanoelectronics, biosensors, solar-cells, catalysis, supercapacitors, etc [3, 4]. Oxidation of graphene (G) to graphene oxide (GO) by introduction of carboxyls, hydroxyls or

epoxide ring in to G backbone is used for tuning their surface hydrophilicity to provide uniform distribution of the carbon nanomaterial in the polymer matrix [5]. This is translated into a decrease of the number of double bonds between carbon atoms and thus decrease of the conjugation length of GO [5]. GO can be partially reduced by chemical, thermal or electrochemical routes generating reduced graphene oxide (RGO), Fig. 1. RGO is a semiconductor of variable energy band gap depending on the extent of reduction, ranging between the insulator GO and the conducting graphene [5].

*Corresponding author e-mail: elsakhawy@yahoo.com

Received 29/1/2020; Accepted 18/2/2020

DOI: 10.21608/ejchem.2020.22915.2375

©2020 National Information and Documentation Center (NIDOC)

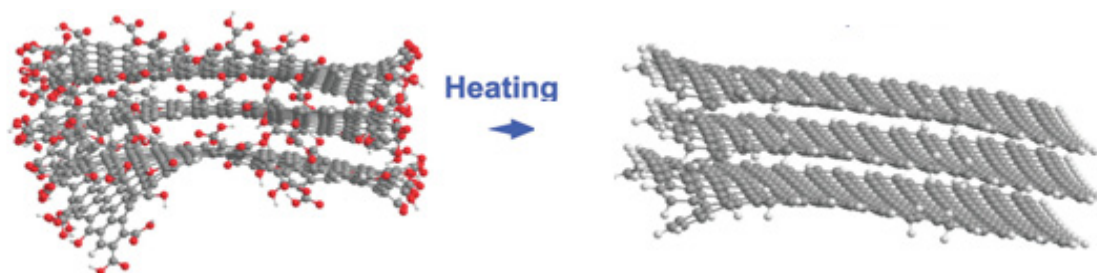


Fig. 1. Visualization of the distortions of graphene edges and their relaxation to the planar state after thermal reduction. The positions of C, H, and O atoms are denoted by grey, white and red balls, respectively [4].

GO is a non-stoichiometric compound; therefore, the carbon-to-oxygen (C/O) ratio depends on the method of preparation and by how much the material is reduced [6]. Before GO can be used in most technological applications, it is important to understand its thermal stability and reduction kinetics [4, 6]. The thermal properties of GO are dependent on its oxygen content [7]. As far as we know, there have been relatively few studies have focused on the thermal stability of GO from different sources [6]. We can apply our algorithm to solve this problem. To illuminate this uncharted area, we studied thermal properties of GO prepared from different agro wastes such as sugarcane bagasse (SCB), rice straw (RS), lignin (L), and mature beech pinewood sawdust (MW).

Thermogravimetric analysis (TGA) is a method that records sample weight loss against temperature under controlled heating rate and inert atmosphere. Differential thermogravimetric analysis (DTA) curves result from TGA curves, and are applied to evaluate the pyrolysis kinetics of biomass [8]. Biomass pyrolysis could be defined as the direct thermal decomposition of organic matter in the absence of oxygen to obtain solid, liquid and gaseous products [2, 9]. In continuation of our previous study on the properties of GO from different agro wastes [10], a thermal decomposition has been discussed here. This analysis was carried out by TGA/ DTA, and the results of these tests have been interpreted with Coates–Redfern method to calculate the activation energy (E_a) of the decomposition reaction.

Experimental

Materials

Sugarcane bagasse (SCB) and black liquor

(BL) were kindly provided from Quena Company for Paper Industry, Egypt. The rice straw (RS) from the Nile valley, harvested in October was used for this study. The straw (leaves and stems) were collected and the seeds were separated. Mature beech pinewood sawdust (MW) was obtained from local wood processing factory. The lignocellulosic materials (SCB, RS, MW, and L) were air dried, homogenized to avoid compositional differences between batches. SCB, RS, and MW were grinding to mesh size 450 micron. Ferrocene (F) was purchased from Sisco research laboratories Pvt. Ltd. Other chemicals used were of analytical grades and used without further purification. Lignin (L) was precipitated from BL by acidic neutralization using 1N HCl, and then filtered; washed with distilled water and air dried. GO was prepared from SCB, RS, L, and MW in the presence and absence of F by the method explained previously in detail [9, 11]. Synthesized GO denoted as SCB/ F, SCB, RS/ F, RS, L/ F, L, MW/F, and MW, respectively.

Thermogravimetric analysis (TGA/ DTA)

TGA studies were carried out on the prepared polymer powders by using a Perkin Elmer thermogravimetric analyzer with nitrogen as purge gas. The specimen was heated to 1000 °C at 10 °C/min in nitrogen atmosphere.

Kinetics of thermal decomposition of SCB/ F, SCB, RS/ F, RS, MW/ F, MW, L/ F, and L, respectively

Thermogravimetric analysis data can be investigated to calculate the activation energy of the thermal degradation process. The general correlation equations used in the Coats–Redfern method are:

$$\log \left[\frac{1 - (1 - \alpha)^{1-n}}{T^2(1-n)} \right] = \log \frac{AR}{\beta E} \left[1 - \frac{2RT}{E} \right] - \frac{E}{2.303RT} \quad \text{for } n \neq 1 \quad (1)$$

$$\log \left[\frac{-\log(1-\alpha)}{T^2} \right] = \log \frac{AR}{\beta E} \left[1 - \frac{2RT}{E} \right] - \frac{E}{2.303RT} \quad \text{for } n = 1 \quad (2)$$

where α is the fractional conversion, n is the order of degradation reaction, R is the gas constant (in kJ/mol.K), T is the temperature (in K), A is the frequency factor (s^{-1}), β is the heating rate (K/min) and E is the activation energy. From the above equation, plotting $\{\log_{10} [1-(1-\alpha)^{1-n}]/T^2(1-n)\}$ against $1/T$ using different n values should offer a straight line, with the most proper value of n . Thus, the method of least squares was applied for the equation, taking various n values (from 0 to 3.0) and calculating for each value of

n , the correlation coefficient (r) and standard error estimation (SE). The activation energies were estimated from the slope ($E/2.303R$), while A were estimated from the intercept ($\log AR/\beta E$) of the Coats–Redfern equation with the most proper value of n , as shown in Fig. 3.

The other kinetic parameters; the enthalpy of activation (H), the entropy of activation (S), and the free energy change of activation (G) were calculated using the relationships:

$$\Delta H^* = E^* - RT; \Delta G^* = \Delta H^* - T\Delta S^* \text{ and } \Delta S^* = 2.303 \left(\log \frac{Ah}{KT} \right) R \quad (3)$$

where (k) and (h) are Boltzman and Planck constants, respectively [12].

Results and Discussion

Thermogravimetric analysis (TGA) and differential thermogravimetric analysis (DTA)

The thermal parameters for each reaction stage were determined from thermal analysis curves as the initial (T_i) and final (T_f) temperatures of decomposition, and (m) temperature peak at maximum rate of weight loss [9].

The TGA curves for SCB/ F, SCB, RS/ F, RS, L/ F, L, MW/F, and MW are given in Fig. 2. In general, the SCB/F, RS/F, L/F, L, and MW/F decomposition curves revealed three decomposition steps, while SCB, RS, and MW revealed two decomposition steps. The difference in the chemical composition of SCB/ F, SCB, RS/ F, RS, L/ F, L, MW/F, and MW causes the observed differences in thermal decomposition behavior and thermal stability. A sudden change in temperature generates a thermal shock and functionalities are taken out from the GO lattice as water vapor, CO, and CO₂. Evolution of gases generates pressure between two GO stacked layers which is the key factor for exfoliation [7].

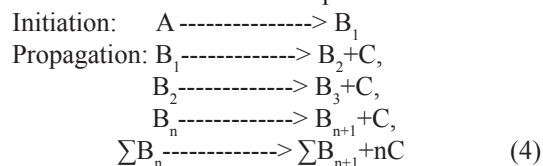
Thermogravimetric curves of SCB, and MW

The TGA/DTA data of SCB and MW are summarized in Table 1. The TGA of SCB, and MW showed a weight loss of 99.87, and 38.91%, respectively, at 1000 °C, which indicated that SCB, and MW contain a fraction of non-volatile components [12]. As shown in Table 1, the residual

weight of SCB was very low; this indicates its high purity and absence of inorganic residues [9].

As shown in Fig. 2b, h, the thermal decomposition processes of SCB, and MW could be divided into two major reaction steps, where the first weight loss was between 36.89-109.5, and 37.23-256.0 °C, with a maximum at 50.27, and 42.97°C (with average weight loss of 14.21, and 7.747 %), respectively, was likely caused by the loss of moisture content [13]. This first weight loss was followed by the main decomposition stage between 109.7-993.0, and 256.1-992.9 °C, with a maximum at 537.6, and 315.4 °C (with average weight loss of 85.66, and 31.16%) for SCB, and MW, respectively. The main weight losses were assigned to fragmentation associated with the pyrolytic decomposition, leading to the formation of aromatized units and the decomposition of the carbonaceous residues [9]. The second reaction involved pyrolytic decomposition by breaking of glucosidic bonds and the linear molecules were converted to lower molecular weight molecules. This latter depolymerization type was considered as the propagation step [9].

The mechanism can be represented as:



where A denotes initial molecules of SCB, RS, or MW; B_1, B_2, \dots, B_n are fragmented molecules; and C denotes volatile products.

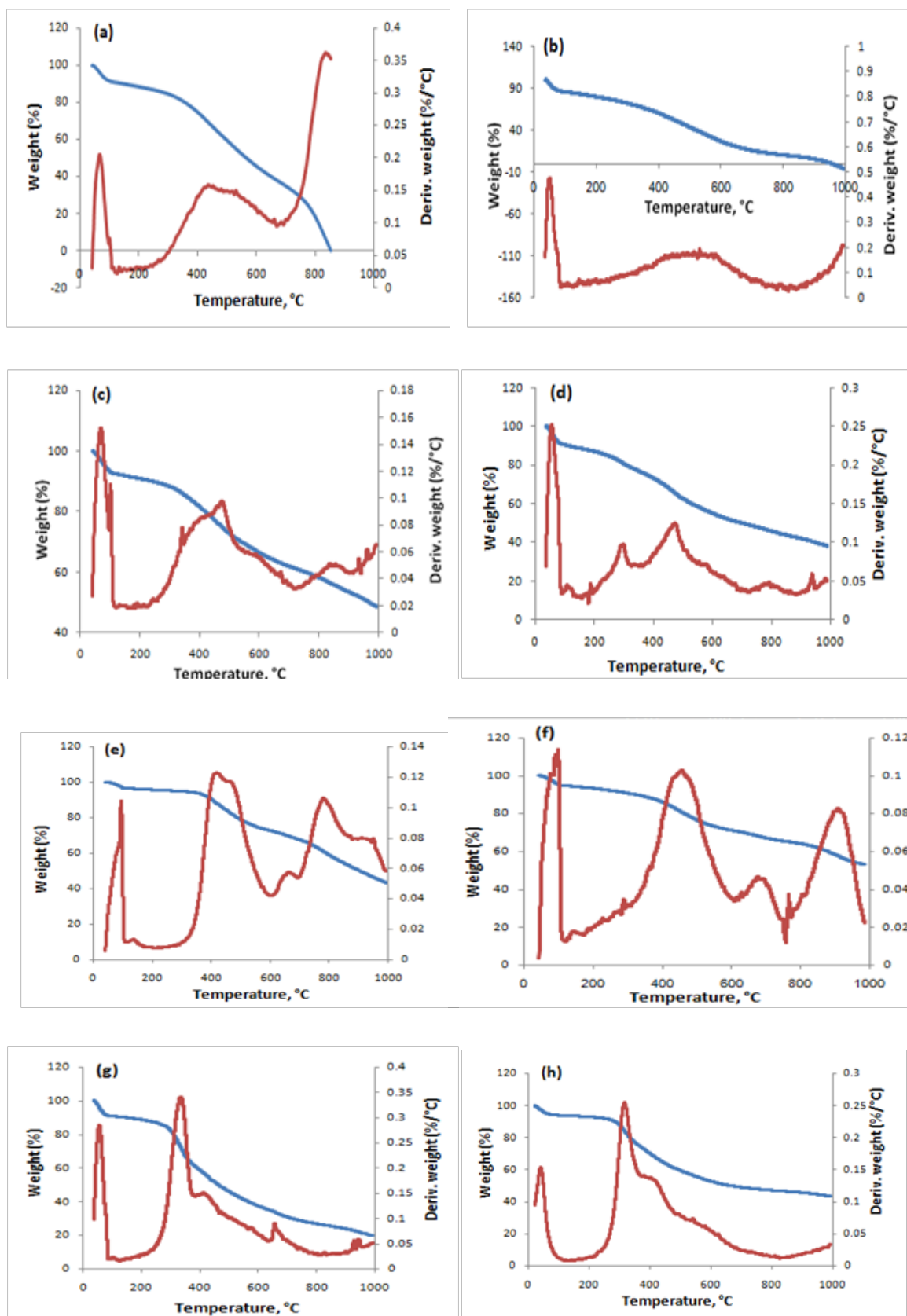


Fig. 2. TGA and DTA curves of (a) SCB/ F, (b) SCB, (c) RS/ F, (d) RS, (e) L/ F, (f) L, (g) MW/ F, and (h) MW, respectively.

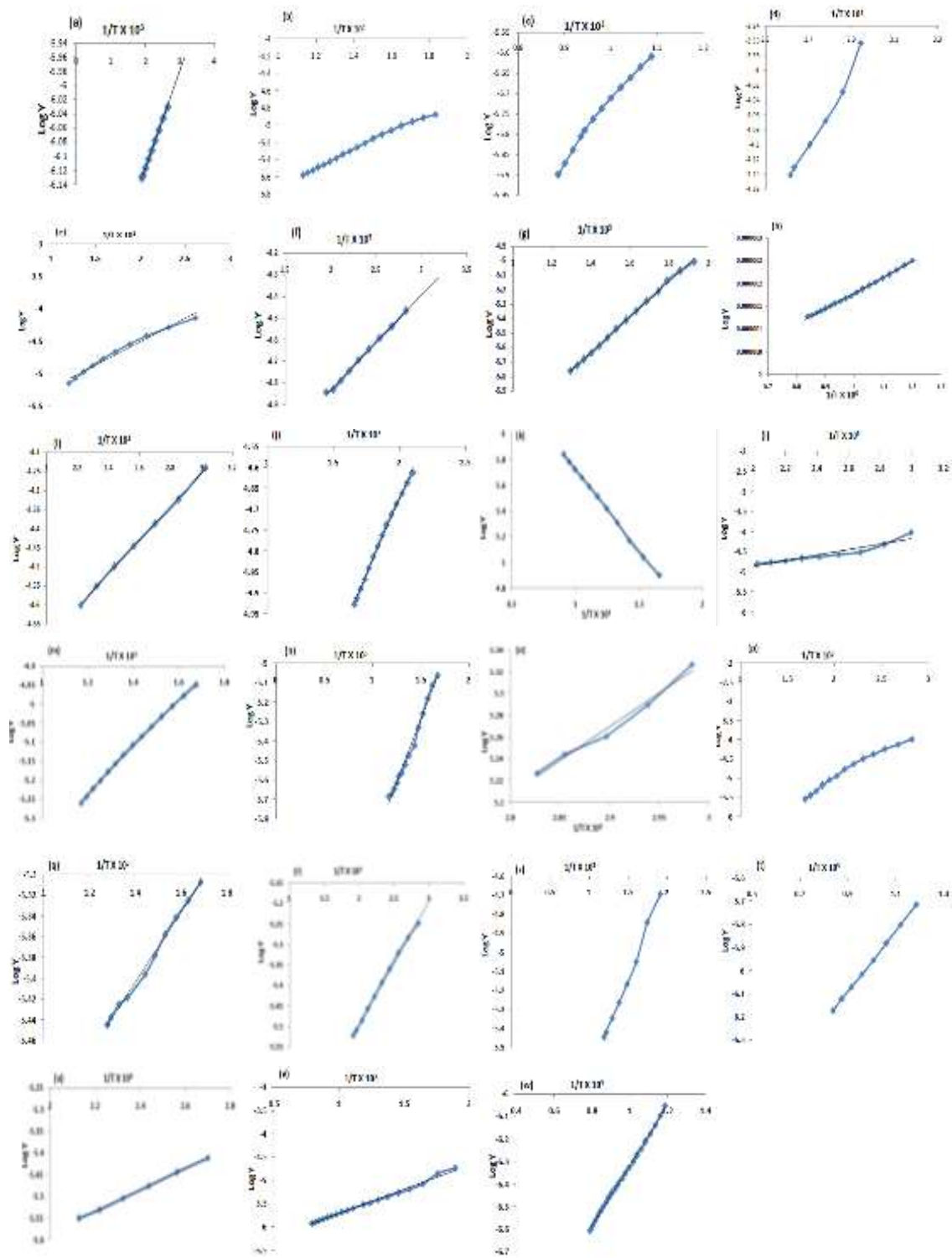


Fig 3. Thermograms of a) 1st, b) 2nd, c) 3rd stages of SCB/ F; d) 1st, e) 2nd stages of SCB; f) 1st, g) 2nd, h) 3rd stages of RS/ F; i) 1st, j) 2nd, k) 3rd stages of RS; l) 1st, m) 2nd, n) 3rd stages of L/ F; o) 1st, p) 2nd, q) 3rd stages of L; r) 1st, s) 2nd, t) 3rd stages of MW/ F; and u) 1st, v) 2nd, w) 3rd stages of MW, respectively.

TABLE 1. TGA data of SCB/ F, SCB, RS/ F, RS, L/ F, L, MW/ F, and (h) MW, respectively.

Sample	Weight loss at 1000 °C, %	Residual weight, %	Temp. of steps in TGA, °C		
			Step 1	Step 2	Step 3
SCB/ F	76.80	23.20	64.64	431.7	836.3
SCB	99.87	0.130	50.27	537.6	-
RS/ F	51.47	48.53	69.61	475.3	838.4
RS	61.62	38.38	56.09	299.8	474.0
L/ F	56.58	43.43	95.12	413.6	779.8
L	46.83	53.17	99.81	457.7	910.1
MW/F	80.26	19.74	56.13	335.3	657.2
MW	38.91	61.09	42.97	315.4	-

The DTA curves of SCB, RS, and MW show two separate endothermic processes. The maxima of the first endotherms appear at 50.27, 56.09, and 42.97 °C for SCB, RS, and MW, respectively, which can be attributed to water evaporation. Meanwhile, the second endotherm with peak maxima appearing at 537.6, 474.7, and 315.4 °C for SCB, and MW, respectively, can be attributed to pyrolytic fragmentation [9].

The weight loss of the GO samples was due to the decarboxylation of carboxylic groups and the loss of CO₂. The conversion of agricultural wastes to GO in the presence and absence of ferrocene affects both the molecular structure and bonding energy, which in turn causes the different thermal behavior of SCB/ F, SCB, RS/ F, RS, L/ F, L, MW/ F, and MW. This finding concurs with another study on bagasse, which concluded that the onset degradation temperature of bagasse decreased as a result of chemical modifications [13].

Thermogravimetric curves of SCB/ F, RS/ F, RS, L/ F, L, and MW/ F

The TGA/DTA data of SCB/ F, RS/ F, RS, L/ F, L, and MW/ F are summarized in Table 1. The TGA of SCB/ F, RS/ F, RS, L/ F, L, and MW/ F showed a weight loss of 76.8, 51.47, 56.09, 56.58, 46.83, 80.26%, respectively, at 1000°C, which indicated that the presence of a fraction of non-volatile components [9].

The thermal decomposition process of SCB/ F, RS/ F, RS, L/ F, L, and MW/ F could be recognized by the three main reaction steps. The initial weight loss of SCB/ F, RS/ F, RS, L/ F, L, and MW/ F between 45.11-252.7, 40.54-245.2, 37.39-202.3, 60.97-323.8, 37.23-80.74, and 37.23-249.1°C, with a maximum at 64.64, 69.61, 56.09, 95.12,

99.81, and 56.13 °C (average weight loss of 13.20, 9.969, 25.04, 5.535, 5.341, and 12.79%), respectively, was likely caused by the loss of moisture content [9]. The second weight loss between 252.9-627.1, 245.3-559.1, 202.6-329.4, 323.9- 581.5, 80.75- 319.9, and 249.2- 569.5, with a maximum at 431.7, 475.3, 299.8, 413.6, 457.7, and 335.3 °C (average weight loss of 44.18, 21.16, 17.36, 21.03, 23.82, and 47.38 %) for SCB/ F, RS/ F, RS, L/ F, L, and MW/ F, respectively, was the result of several coincident processes, such as dehydroxylation, combined with pyrolytic fragmentation, leading to the development of aromatized units and volatile products [9]. In another words, pyrolysis of the most labile oxygen functional groups such as hydroxyl groups had occurred, which then released CO, CO₂ and steam in the second decomposition step [14]. The third decomposition step between 647.3-855.2, 559.3-992.6, 366.6-830.0, 323.9-591.5, 320-508.9, and 569.7-992.9 °C, with a maximum at 836.3, 838.4, 474.0, 779.8, 910.1, and 657.2 (average weight loss of 19.42, 20.34, 19.22, 30.01, 17.67, and 20.09 %), which was ascribed to the decomposition of the carbonaceous residues to form low molecular weight gaseous products, i.e., the thermal decomposition was likely related to the combustion of the crosslinked aromatized units formed in the 2nd step [9].

The lower rate of weight lost over temperature in the final region may be due to the burning of more stable oxygen functionalities i.e. the double bond between carbon and oxygen of the carboxyl group [14].

These three steps may match the three steps suggested by Chatterjee as representing the thermal degradation [9]:

First step: $A_1 \text{-----} \rightarrow B_1$ volatile product or dehydration.

Second step: $B_1 \text{-----} \rightarrow B_2 + C$,
 $B_2 \text{-----} \rightarrow B_3 + C$, thermal degradation

$\sum B_n \text{-----} \rightarrow \sum B_{n+1} + C$,

Third step: $\sum B_n \text{-----} \rightarrow$ carbonization (ash). (5)

where A denotes the initial molecules of SCB/ F, RS/ F, L/ F, L, and MW/ F; B_1, B_2, \dots, B_n are fragmented molecules and C represents volatile products.

The DTA of SCB/ F, RS/ F, RS, L/ F, L, and MW/ F shows three endothermic Processes. The maxima of the first endotherms appear at 64.64, 69.61, 56.09, 95.12, 99.81, and 56.13°C for SCB/ F, RS/ F, RS, L/ F, L, and MW/ F, respectively, which can be attributed to water evaporation. Meanwhile, the second endotherm with peak maxima appearing at 431.7, 475.3, 299.8, 413.6, 457.7, and 335.3°C for SCB/ F, RS/ F, RS, L/ F, L, and MW/ F, respectively, can be attributed to the splitting of polymer main chain [9, 15]. Third endothermic peak maxima appearing at 836.3, 838.4, 474.0, 779.8, 910.1, and 657.2 ascribed to the decomposition of the polymer backbone [15]. The endothermic temperatures for MW/ F, and RS shifted towards lower values than that of SCB/ F, RS/ F, L/ F, and L. This shift showed that MW/ F, and RS samples were less thermally stable in contrast to other agrowastes treated with F [9]. This may be due to the decrease of double bond oxygen content (discussed in FTIR section).

From the short review above, key findings emerge that SCB/ F, RS/ F, L/ F, and MW/ F are higher thermal stable than SCB, and MW may be due to the effect of F towards thermal stabilization. While untreated L's thermal stability may be due to α - and β - aryl-alkyl-ether linkages [16].

This recommendation based on the following evidences:

(i) the increase in the DTG peak temperature of the first and second decomposition peaks of SCB/ F, RS/ F, L/ F, L, and MW/ F samples (from 50.27 to 99.81 °C and from 335.3 to 475.3 °C) over SCB, RS, and MW (from 42.97 to 56.09 °C and from 315.4 to 537.6 °C); (ii) the reduction in weight loss, where the weight loss of the first peak is decreased. This means that the volatilization stage of decomposition is slowest occurred, in case of SCB/ F, RS/ F, L/ F, L and MW/ F than SCB, RS, and MW; and (iii) the increase in the calculated activation energy ($\sum E_a$) of SCB/ F, RS/ F, L/ F, L

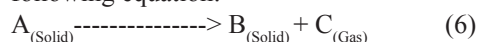
and MW/ F. The high production of char residue from MW, and L pyrolysis can be ascribed to its lower content of methoxyl group (determined by FTIR) [17].

Finally, the TGA results imply that the mobility of the polymer segments in SCB/ F, RS/ F, L/ F, and MW/ F was suppressed by the strong hydrogen bonding interactions between them, resulting in a delay in the polymer degradation [15]. Overall, the thermal stability of the GO treated with F has been improved compared to that of pure GO without F, confirming the positive structural changes.

Furthermore, the nanostructure of GO can form lots of localized hotspots where energy is localized, consequently, this nanostructure also cause the thermal decomposition process occur in advance as in SCB/ F compared to other agrowastes treated with F [18].

Kinetics of thermal decomposition of SCB/ F, SCB, RS/ F, RS, MW/ F, MW, L/ F, and L, respectively

Generally, the thermal decomposition of polymeric materials can be symbolized by the following equation:



E_a values increased in SCB/ F, RS/ F, L/ F, and MW/ F compared to SCB, RS, L, and MW due to the decreased disorder inside the SCB, and MW matrix [9, 15]. This enhancement in E_a is a good indication of higher thermal stability for the GO treated with F compared to the pure GO. This result implies that the current SCB/ F, RS/ F, L/ F, and MW/ F are a suitable material for using in potential applications.

On the other hand by comparing between GO treated with F .i.e. SCB/ F, RS/ F, L/ F, and MW/ F, it was previously shown that E_a for the decomposition of functional groups strongly depends on the matrix structure. In our case there may be several explanations for the lowering of E_a (i.e. SCB/ F) with the increase in oxygen content (discussed in FTIR section [10]). Firstly, functional groups distort the surface leading to stresses. Thus, because of higher oxygen content and stresses on the SCB/ F surface, the distorted planes at the edges of the nanoflakes are prone to relaxation (Fig. 1). Secondly, functional groups facilitate the decomposition of each other by a kind of autocatalytic effect (for example, decarboxylation of salicylic acid takes place at

TABLE 2. Thermoanalytical and thermodynamic data of the thermal decomposition steps of SCB/F, SCB, RS/F, L, MW/F, and MW samples.

Sample	Stage	TGA range C°	DTA peak C°	Mass %, loss	n	R ²	(A (s ⁻¹))	(KJ mol ⁻¹)	(KJ mol ⁻¹)	SE	E _a (kJ mol ⁻¹)
SCB/F	1 st	252.7-45.11-	64.64	13.20	0	0.999	19.53	-0.06	-0.221	0.000746	2.63
	2 nd	627.1-252.9-	431.7	44.18	1.5	0.995	14.33	17.30	-0.223	0.016251	19.99
	3 rd	855.2-647.3-	836.3	19.42	1.5	0.995	15.17	17.71	-0.253	0.004638	24.45 E=47.07Σ
SCB	1 st	109.5-36.89-	50.27	14.21	1.5	0.949	10.90	9.59	-0.226	0.025686	12.28
	2 nd	993.0-109.7-	537.6	85.66	1.5	0.979	11.16	11.04	-0.226	0.052001	13.73 E=26.01Σ
RS/F	1 st	245.2-40.54-	69.61	9.969	1.5	0.951	12.05	9.02	-0.225	0.053374	11.86
	2 nd	559.1-245.34-	475.3	21.16	2	0.998	17.90	21.18	-0.229	0.009719	27.40
	3 rd	992.6-559.3-	838.4	20.34	0.5	0.996	13.43	3.49	-0.234	0.002133	12.73 E=51.99Σ
RS	1 st	202.3-37.39-	56.09	25.04	1.5	0.999	10.57	6.61	-0.226	0.003365	9.34
	2 nd	202.6-329.4	299.8	17.36	1.5	0.995	11.95	7.51	-0.232	0.0067	13.73
	3 rd	366.6-830.0	474.0	19.22	2	0.999	15.29	17.98	-0.230	0.09146	24.196 E=47.266Σ
L/F	1 st	323.8-60.97-	95.12	5.535	1.5	0.942	12.27	9.29	-0.226	0.069097	12.35
	2 nd	581.5-323.9-	413.6	21.03	0.5	0.997	11.65	6.14	-0.231	0.005176	11.84
	3 rd	591.5-323.9-	779.8	30.01	1.5	0.994	16.77	17.41	-0.232	0.017433	26.16 E=50.35Σ
L	1 st	80.74-37.23-	99.81	5.341	0.5	0.902	0.48	19.33	-0.253	0.043842	22.43
	2 nd	319.92-80.75-	457.7	23.82	2.5	0.977	20.43	20.75	-0.227	0.081883	26.82
	3 rd	508.93-320-	910.1	17.67	0.5	0.996	12.59	-3.37	-0.235	0.003059	6.47 E=55.72Σ
MW/F	1 st	249.1-37.23-	56.13	12.79	0.5	0.997	14.18	2.99	-0.224	0.004686	5.73
	2 nd	569.5-249.2-	335.3	47.38	1.5	0.995	14.08	14.99	-0.229	0.020787	20.04
	3 rd	992.9-569.7-	657.2	20.09	2.5	0.999	16.84	17.46	-0.231	0.00228	25.19 E=50.96Σ
MW	1 st	256.1-37.23-	42.97	7.747	0.5	0.998	0.07	3.31	-0.267	0.003613	5.94
	2 nd	992.9-256.1-	315.4	31.16	1.5	0.998	14.40	15.11	-0.228	0.027521	20.00 E=25.94Σ

much lower temperatures than that of benzoic acid). Therefore, their larger amount makes the decomposition easier and faster. These effects are clearly seen for keto/hydroxy acids and carboxyls because these groups dominate at the oxidized carbon surface. They are the strongest acceptors and their presence in the carbon material leads to the distortions and stresses in the G layers. In the case of SCB/F this effect looks more possible because of the higher defectiveness [4].

G of this system is positive. Consequently, the thermodynamics of GO should be non spontaneous, which implies that the thermal reduction can occur under relative high-temperature conditions [19]. This result implies that the current nanocomposite is a suitable material for using in potential applications. Higher E_a observed for L, and RS is may be due to the lower amount of oxygen moieties present [20].

Analyzing the thermal degradation kinetics, it has been found that thermal degradation of GOs order reaction is different, i.e., the rate of reaction is ranging from 0 to 3 depending on the agrowaste source and F using. E_a determined for thermal reduction of GOs are found to be from 21.00 to 55.35 kJ/mol. From TGA, it was found that the rate of removal of oxygen-containing functional groups depends on the temperature, which agrees with the experimental findings and thermal degradation kinetics. The lower rate of weight lost over temperature in the final region may be due to the burning of more stable oxygen functionalities i.e. the double bond between carbon and oxygen of the carboxyl group [14].

Conclusion

The analysis leads to the following conclusions:

1. The thermal decomposition process of SCB, and MW could be divided into two major reaction steps, where the first weight was between 36.89-109.5, and 37.23-256.0 °C, with a maximum at 50.27, and 42.97°C (with average weight loss of 14.21, and 7.747 %), respectively, was likely caused by the loss of moisture content. The second main decomposition stage was between 109.7-993.0, and 256.1-992.9 °C, with a maximum at 537.6, and 315.4 °C (with average weight loss of 85.66, and 31.16%) for SCB, and MW, respectively due to fragmentation associated with the pyrolytic decomposition, leading to the formation of aromatized units and the decomposition of the carbonaceous residues.

Calculated E_a was 26.01 and 25.94 for SCB, and MW, respectively.

2. The thermal decomposition process of SCB/F, RS/F, RS, L/F, L, and MW/F could be recognized by the three main reaction steps. The initial weight loss of SCB/F, RS/F, RS, L/F, L, and MW/F was between 45.11-252.7, 40.54-245.2, 37.39-202.3, 60.97-323.8, 37.23-80.74, and 37.23-249.1°C, with a maximum at 75, 75, 69.61, 56.09, 95.12, 99.81, and 56.13°C (average weight loss of 13.20, 9.969, 25.04, 5.535, 5.341, and 12.79%), respectively, was likely caused by the loss of moisture content. The second main weight loss between 252.9-627.1, 245.3-559.1, 202.6-329.4, 323.9- 581.5, 80.75-319.9, and 249.2- 569.5, with a maximum at 431.7, 475.3, 299.8, 413.6, 457.7, and 335.3 °C (average weight loss of 44.18, 21.16, 17.36, 21.03, 23.82, and 47.38 %) for SCB/F, RS/F, RS, L/F, L, and MW/F, respectively, was the result of dehydroxylation, combined with pyrolytic fragmentation. The third decomposition step between 647.3-855.2, 559.3-992.6, 366.6-830.0, 323.92-591.5, 320-508.9, and 569.7-992.9 °C, with a maximum at 836.3, 838.4, 474.0, 779.8, 910.1, and 657.2 (average weight loss of 19.42, 20.34, 19.22, 30.01, 17.67, and 20.09 %), which was ascribed to the decomposition of the carbonaceous residues to form low molecular weight gaseous products. Calculated E_a was 47.07, 40.13, 47.26, 50.35, 55.72, and 50.96 for SCB/F, RS/F, RS, L/F, L, and MW/F, respectively.
3. All the prepared GO have positive G which means non spontaneous reaction.

References

1. Fahmy, Y., Fahmy, T. Y. A., Mobarak, F., El-Sakhawy, M., and Fadel, M. H., Agricultural Residues (Wastes) for Manufacture of Paper, Board, and Miscellaneous Products: Background Overview and Future Prospects. *International Journal of ChemTech Research*, **10**(2), 424-448 (2017).
2. Fahmy, T. Y. A., Fahmy, Y., Mobarak, F., El-Sakhawy, M., and Abou-Zeid, R. E., Biomass Pyrolysis: Past, Present, and Future. *Environment, Development and Sustainability*, **22**(1), 17-32 (2020).
3. Slobodian, O. M., Lytvyn, P. M., Nikolenko,

- A. S., Naseka, V. M., Khyzhun, O. Y., Vasin, A. V., and Nazarov, A. N., Low-temperature reduction of graphene oxide: electrical conductance and scanning Kelvin probe force microscopy. *Nanoscale research letters*, **13**(1), 139 (2018).
- Chernyak, S. A., Ivanov, A. S., Podgornova, A. M., Arkhipova, E. A., Kupreenko, S. Y., Shumyantsev, A. V., and Lunin, V. V., Kinetics of the defunctionalization of oxidized few-layer graphene nanoflakes. *Physical Chemistry Chemical Physics*, **20**(37), 24117-24122 (2018).
 - Nikolakopoulou, A., Tasis, D., Sygellou, L., Dracopoulos, V., Galiotis, C., and Lianos, P., Study of the thermal reduction of graphene oxide and of its application as electrocatalyst in quasi-solid state dye-sensitized solar cells in combination with PEDOT. *Electrochimica Acta*, **111**, 698-706 (2013).
 - Jung, I., Field, D. A., Clark, N. J., Zhu, Y., Yang, D., Piner, R. D., and Ruoff, R. S., Reduction kinetics of graphene oxide determined by electrical transport measurements and temperature programmed desorption. *The Journal of Physical Chemistry C*, **113**(43), 18480-18486 (2009).
 - Sengupta, I., Chakraborty, S., Talukdar, M., Pal, S. K., and Chakraborty, S., Thermal reduction of graphene oxide: How temperature influences purity. *Journal of Materials Research*, **33**(23), 4113-4122 (2018).
 - El-Gendy, A., Abou-Zeid, R. E., Salama, A., Diab, M. A., and El-Sakhawy, M., TEMPO-oxidized cellulose nanofibers/polylactic acid/TiO₂ as antibacterial bionanocomposite for active packaging. *Egyptian Journal of Chemistry* **60** (6) 1007-1014 (2017).
 - El-Sakhawy, M., Tohamy, H. A. S., Salama, A., and Kamel, S., Thermal properties of carboxymethyl cellulose acetate butyrate. *CELLULOSE CHEMISTRY AND TECHNOLOGY*, **53**(7-8), 667-675 (2019).
 - Tohamy, H. A. S., Anis, B., Youssef, M. A., Abdallah, A. E. M., El-Sakhawy, M., and Kamel S., Preparation of eco-friendly graphene oxide from agricultural wastes for water treatment. *Desalination and Water Treatment*, **191**, 250-262 (2020).
 - Somanathan, T., Prasad, K., Ostrikov, K. K., Saravanan, A., and Krishna, V. M., Graphene Oxide Synthesis from Agro Waste. *Nanomaterials*, **5**, 826-834 (2015).
 - Adel, A. M., El-Wahab, Z. H. A., Ibrahim, A. A., & Al-Shemy, M. T., Characterization of microcrystalline cellulose prepared from lignocellulosic materials. Part II: Physicochemical properties. *Carbohydrate Polymers*, **83**(2), 676-687 (2011).
 - El-Sakhawy, M., Kamel, S., Salama, A., Youssef, M.A., Teyor, W.E., and Tohamy, H.-A.S., Amphiphilic Cellulose as Stabilizer for Oil/Water Emulsion, *Egyptian Journal of Chemistry* **60**(2) 181-204 (2017).
 - Yusoff, N., Synthesis of functionalized graphene/copper oxide (CuO) nanocomposites and their catalytic activity, Masters thesis, Malaya University, Kuala Lumpur (2013).
 - Yassin, A. Y., Mohamed, A. R., Abdelrazek, E. M., Morsi, M. A., and Abdelghany, A. M., Structural investigation and enhancement of optical, electrical and thermal properties of poly (vinyl chloride-co-vinyl acetate-co-2-hydroxypropyl acrylate)/graphene oxide nanocomposites. *Journal of Materials Research and Technology*, **8**(1), 1111-1120 (2019).
 - Schniewind, A. P., Concise encyclopedia of wood & wood-based materials. MIT Press (1989).
 - Zhao, J., Xiuwen, W., Hu, J., Liu, Q., Shen, D., and Xiao, R., Thermal degradation of softwood lignin and hardwood lignin by TG-FTIR and Py-GC/MS. *Polymer degradation and stability*, **108**, 133-138 (2014).
 - Zeng, G. Y., Zhou, J. H., and Lin, C. M., The thermal decomposition behavior of graphene oxide/HMX composites. In *Key Engineering Materials*, **645**, 110-114. Trans Tech Publications Ltd (2015).
 - Yin, K., Li, H., Xia, Y., Bi, H., Sun, J., Liu, Z., and Sun, L., Thermodynamic and kinetic analysis of low temperature thermal reduction of graphene oxide. *Nano-Micro Letters*, **3**(1), 51-55 (2011).
 - Phiri, J., Johansson, L. S., Gane, P., and Maloney, T., A comparative study of mechanical, thermal and electrical properties of graphene-, graphene oxide- and reduced graphene oxide-doped microfibrillated cellulose nanocomposites. *Composites Part B: Engineering*, **147**, 104-113 (2018).

الخواص الحرارية لأكسيد الجرافين المحضرة باستخدام الفيروسين من النفايات الزراعية المختلفة

هبة الله سرحان تهاى¹، سمير كامل¹، محمد السخاوى¹، محمد عادل يوسف²، اميرة عبدالله²، بدوى انيس³
¹ قسم السليلوز والورق، المركز القومى للبحوث
² قسم الكيمياء، كلية العلوم، جامعة حلوان
³ قسم الطيف، شعبة الطبيعة، المركز القومى للبحوث

أكسيد الجرافين (GO) المستخرج من النفايات الزراعية المختلفة مثل قصب قصب السكر (SCB) ، قش الأرز (RS) ، اللجنين (L) ، نشارة خشب الصنوبر (MW) في وجود وغياب الفيروسين كعامل مساعد عند 300 °C تم إعدادها وتقييمها بواسطة TGA و DTA. وأظهرت منحنيات TGA التحلل ل GO في ثلاث مراحل باستثناء GO التي أعدت من SCB ، ومن MW في غياب الفيروسين حيث مرت بمرحلتين للتحلل. كان الوزن المتبقي ل SCB منخفضًا جدًا ؛ هذا يدل على درجة نقاء عالية وغياب المخلفات غير العضوية. يمكن أن يُعزى الإنتاج العالي لمخلفات الرماد من MW و L بالانحلال الحراري إلى محتواها الأقل من مجموعة الميثوكسيل (تم تحديدها بواسطة FTIR). تم حساب طاقة التنشيط (Ea) ل GO لتكون من 21.00 إلى 55.35 كيلو جول / مول. من TGA ، وجد أن معدل إزالة المجموعات الوظيفية المحتوية على الأكسجين يعتمد على درجة الحرارة ، والتي تتفق مع النتائج التجريبية وحركية التحلل الحراري. تغيير الطاقة الحرة للتفعيل (GA) لهذا النظام كان إيجابيًا. وبالتالي ، يجب أن تكون الديناميكا الحرارية ل GO غير تلقائية.